

ASPECTS OF EQUIVALENCE IN TWO-DIMENSIONAL RESISTIVITY IMAGING AND MODELLING

A.I. Olayinka

Department of Geology, University of Ibadan, Ibadan
E-mail olayinka@ibadan.skannet.com

Received 28 June 1997; Revision accepted 1 July, 1999

ABSTRACT

The possibility for geoelectrical equivalence in two-dimensional (2-D) inversion of apparent resistivity data has been investigated. This involved the calculation of synthetic pseudosection data for simple geological structures using a finite difference approach. With the aid of statistical F-test, it is shown that identical or near-identical pseudosections can be generated from more than one 2-D model. In particular, the apparent resistivity pseudosection measured over 2-D structures like basement fault, trough and horst resemble those arising from lateral variations in the overburden resistivity.

INTRODUCTION

During the past decade or so, highly sophisticated computer-controlled multi-electrode resistivity measurement systems have been successfully developed, capable of a high data density needed for a two-dimensional (2-D) electrical imaging of the subsurface (Griffiths and Turnbull, 1990; Dahlin, 1993). Such systems are very useful in evaluating the groundwater resource potential of weathered and fractured crystalline basement rocks (Olayinka and Barker, 1990; Griffiths and Barker, 1993), as well as for engineering and environmental investigations (Bernstone and Dahlin, 1997). Softwares are now available for data inversion and imaging, thus facilitating interpretation of the data (Barker, 1992; Loke and Barker, 1996).

It is widely appreciated that the interpretation of geophysical data is hardly unique with more than one geologic model fitting the same set of field observations. On one hand, the subject of electrical equivalence in the 1-D inversion of resistivity sounding data has received considerable attention in the literature (e.g. Koefoed, 1979; Simms and Morgan, 1992; Zhdanov and Keller, 1994). Non-uniqueness in 1-D resistivity inversion arises largely because identical sounding curves can be generated from models that have the same transverse resistance (for resistive layer). Hence, inversion of the data cannot resolve the true layer parameters for sounding curves which differ by only a few per cent. Conversely, most of the inversion algorithms used in geoelectrical tomography have focused largely on the construction of images of the potential distribution and little on the uncertainty, or non-uniqueness, of such images, even though

it is recognised that the possibility for equivalence exists in 2-D inversion. The principal objective of the present work, therefore, is to show identical or near-identical apparent resistivity pseudosections that have been generated from different 2-D models. Both Wenner and dipole-dipole data have been modelled.

METHOD

Synthetic apparent resistivity pseudosection data were calculated using a 2-D forward modelling algorithm 2DSIRT developed by Weller et al (1996). The program uses a finite difference approach (Dey and Morrison, 1979) to solve for the potential distribution due to point sources of current. The modelling routine accounts for 3-D sources (current electrodes) in a 2-D material model. This implies that the resistivity can vary arbitrarily along the line of surveying (x-direction) and with depth (z-direction), but the models have an infinite extension along the strike or y-direction. The forward problem for each current source is solved separately and the apparent resistivity for any desired configuration are computed by a superposition of several pole-pole configuration. In the case of multi-electrode arrays this procedure reduces the number of forward problems to the number electrodes, which is generally much lower than the number of measured configurations.

A rectangular grid was used, which coarsens away from the centre of the air-earth interface. Each node on the grid is assigned a particular resistivity. The grid used consists of 129 horizontal nodes and 23 vertical nodes for the Wenner array and 85 horizontal nodes and 23 vertical dipoles for the dipole-dipole array.

Discretization errors, which are caused by the inadequate approximation of the introduction of current at a point by the finite difference grid, are removed considerably by the application of a singularity removal (Lowry et al., 1989). To further improve the accuracy, the minimal and maximal discrete wave numbers are chosen according to the maximal and minimal distances, respectively, between the current and potential electrodes. The precision of the Fourier transform can also be improved by increasing the number of discrete wave numbers per decade. Six wave numbers per decade are used in the present work and gave a sufficient precision.

In the discussion that follows, the calculated apparent resistivities are plotted in terms of the depth of investigation, Z_e , for each electrode array. For the Wenner array (Fig. 1a) this is $0.519a$ (Edward, 1977) where 'a' is the electrode spacing. In the dipole-dipole array (Fig. 1b), where series of measurements are taken with a fixed dipole length 'a' and the dipoles are separated by a variable integral number of dipole lengths 'na', the plotting position is with respect to the distance between the outermost electrodes, L (note: $L = na + 2a$). Z_e varies from about $0.135L$ for $n=1$, through about $0.216L$ for $n=6$ to about $0.239L$ for $n=20$.

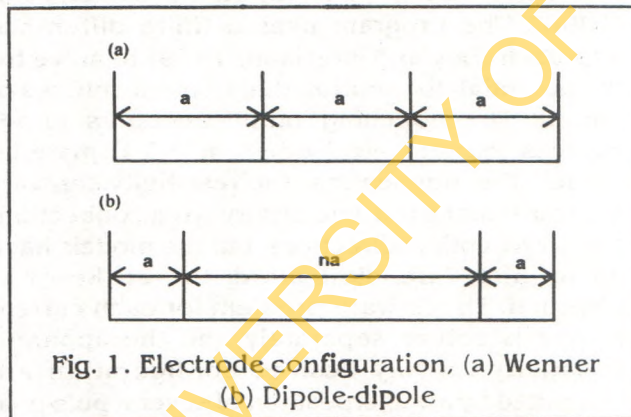


Fig. 1. Electrode configuration, (a) Wenner
(b) Dipole-dipole

The F-ratio was employed as a statistical parameter to measure the equivalence between any two sets of 2-D models. As a first step, the variance of each apparent resistivity pseudosection data is calculated thus (Davies, 1973).

$$S^2 = (1/N-1) \sum (\rho_a(i) - \bar{\rho}_a)^2$$

where N = number of data points

$\rho_a(i)$ = apparent resistivity value at the i th measurement point and $\bar{\rho}_a$ is the mean of all the apparent resistivities. The F-ratio between the two

is determined as

$$F = (S_1)^2 / (S_2)^2$$

where $(S_1)^2$ is the larger variance and $(S_2)^2$ the smaller. For the Wenner data, $N = 472$ and for the dipole-dipole $N = 280$. A 95 per cent confidence interval was chosen, for which the f-table value ($f(V_1, V_2, \alpha)$) is 1.46. V_1 and V_2 are the number of degrees of freedom and α the confidence interval. If the calculated F-ratio is greater than the f-table value, the difference between the two pseudosections is statistically significant, implying that a significantly large amount of the variation in the data about the mean has been taken up by the regression equation (Draper and Smith, 1981).

RESULTS

Fault Model

In the 2-D model of Fig. 2a, the bedrock interface, which is at a depth of 30m, is planar. Along one-half, the overburden resistivity is 50 ohm-m while in the second half the overburden resistivity is 200 ohm-m. The bedrock resistivity is 5000 ohm-m. The Wenner apparent resistivity pseudosection calculated for this structure is presented in Fig. 2b. The resistivity pattern reflects to a large extent the lateral variation in the overburden resistivity, with higher apparent resistivities towards the right hand side of the pseudosection. There is a steepening of the contours in the vicinity of the contact between the low and the high-resistivity section of the overburden, although none of the contours precisely defines the position of the contact.

Intuitively, a contour pattern similar to that in Fig. 2b could be also be expected if the bedrock were to be shallower towards the right hand side while the overburden resistivity is constant. With the overburden and bedrock resistivities fixed at 50 and 5000 ohm-m, respectively, and the depth to the bedrock interface on the right hand side was reduced from 30m and a new pseudosection data set calculated. The new data set was then compared to that in Fig. 2b. After 4 iterations, the buried fault model of Fig. 2c was attained in which the depths to bedrock in the upthrown block is 6.6m. The pseudosection data calculated for this model (Fig. 2d) is similar to that in Fig. 2b, although the zone with apparent resistivities greater than about 600 ohm-m is now wider.

The F-ratio between the two pseudosections is 1.311, which is lower than the value from the f-table. This indicates that the difference between

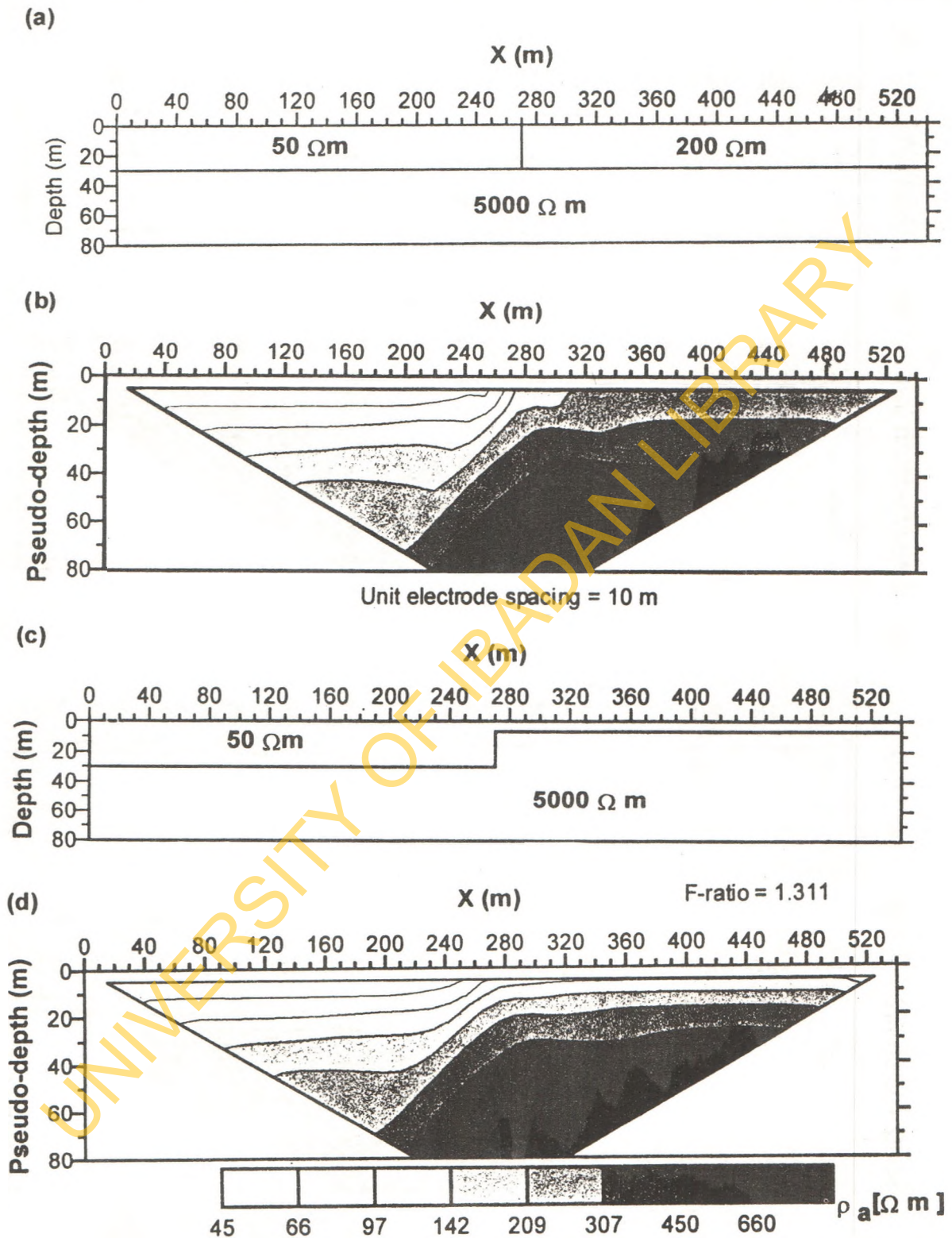


Fig. 2. Example equivalence of 2-D models in a fault (or step) model (Wenner array), (a) 2-D model with lateral variation in resistivity, (b) apparent resistivity pseudosection calculated from (a), (c) 2-D model that is equivalent to the model in (a), (d) apparent resistivity pseudosection data calculated from the fault model in (c)

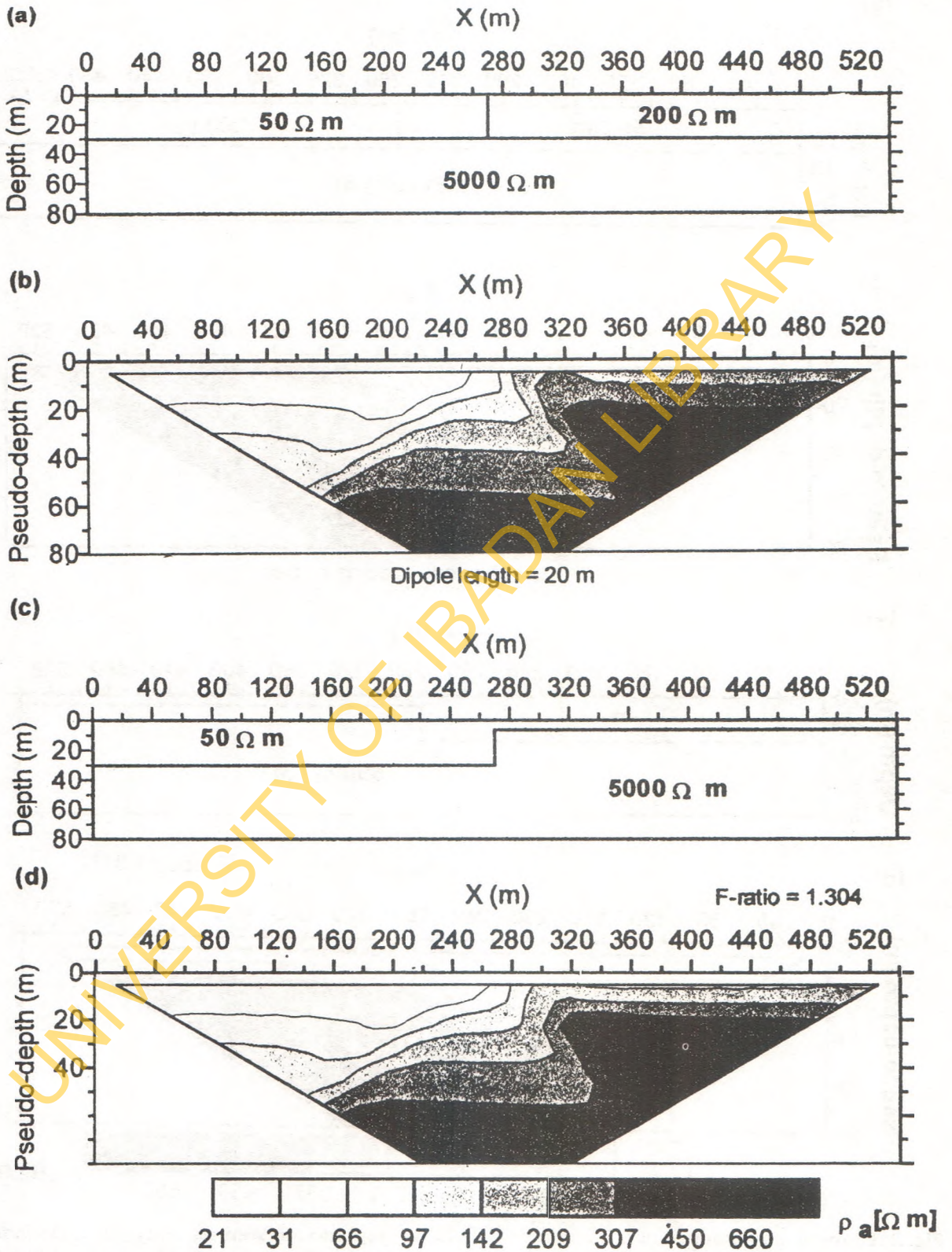


Fig. 3. Example equivalence of 2-D models in a fault structure (Dipole-dipole array), (a) 2-D model with lateral variation in resistivity, (b) apparent resistivity pseudosection calculated from (a), (c) 2-D model that is electrically equivalent to the model in (a), (d) pseudosection data calculated from (c)

the two pseudosections is not statistically significant and hence, a near-equivalence between the two 2-D models in Figs. 2a and 2c could be assumed. Similar results were obtained for the dipole-dipole array (Fig. 3) although in this case the F-ratio between the respective pseudosections is slightly lower at 1.304.

Trough Model

In the 2-D model presented in Figure 4a, there are two vertical contacts; the overburden resistivity at the centre of the model is 50 ohm-m while the resistivity of the remaining part of the overburden is 200 ohm-m. The depth to the bedrock interface is 20m and the bedrock resistivity is 3000 ohm-m. The Wenner apparent resistivity pseudosection calculated for this model (Fig. 4b) shows a low resistivity anomaly at the centre, coinciding with the position of the low resistivity section of the overburden. This pattern of resistivity distribution resembles that for a basement trough structure in which the resistivity of the fill material is less than that of the bedrock. By trial and error adjustment of the model parameters the model in Fig. 4c was attained. The depth to the bottom of the basin is about 49m while the depth to the top is about 4.3m. A comparison between the models in Figs. 4a and 4c shows that there is a 145% increase in the depth to the bedrock interface at the centre of the respective models. The bedrock resistivity was reduced to 2250 ohm-m. The pseudosection data calculated for this structure are presented in Fig. 4d. The F-ratio between the two pseudosections is 1.072, which is not statistically significant at the 95% confidence level.

A dipole-dipole pseudosection was also calculated for a model with two vertical contacts (Fig. 5a) in which the resistivity at the centre is 50 ohm-m while at the flanks the resistivity is much higher at 200 ohm-m. There is a low resistivity structure flanked by highs at shallow levels of the pseudosection (Fig. 5b). However, at depth, there is a resistivity high at the position of the low resistivity structure, flanked by highs. The highest apparent resistivities are of the order of 1000 ohm-m, which is about one-third of the bedrock resistivity. A similar pseudosection (Fig. 2d) was calculated for a basement trough structure (Fig. 5c) in which the depth to the bottom of the

trough is 27 m while at the upthrown block the depth to the interface is 4.6 m. The F-ratio between the two pseudosections is 1.054 which is not statistically significant at the 95% confidence interval. It may be pointed out that in this example the increase in the depth to bedrock interface from Figs. 5a to 5c is much smaller (at about 35%) than for the corresponding case with the Wenner array (see Fig. 4.)

Horst Model

The Wenner apparent resistivity pseudosection measured over a 2-D model (Fig. 6a) in which a high resistivity (200 ohm-m) is flanked by lower resistivity materials (50 ohm-m) is presented in Fig. 6b. The depth to the bedrock interface is 30m while the bedrock resistivity is 3000 ohm-m. The contoured Wenner section reflects, to a very large extent, the resistivity distribution in the model, displaying a resistivity high at the position of the higher resistivity overburden, flanked by resistivity lows. This anomaly pattern resembles what would be expected over a basement ridge. It was decided, therefore, to calculate another pseudosection for a 2-D horst structure, with an overburden resistivity of 50 ohm-m and a bedrock resistivity of 3000 ohm-m.

Only the depth to the top of the horst was adjusted during the iterations. After 4 iteration steps, the pseudosection of Fig. 6d was generated (from the 2-D model shown in Fig. 6c) in which the depth to the top of the horst is 8.5m. This pseudosection resembles the one for a lateral variation in resistivity (Fig. 6b), the main difference being a slight underestimation of apparent resistivity for levels 1 and 2 of the pseudosection. The F-ratio between them is 1.153, which is not statistically significant.

The procedure was repeated for the dipole-dipole array. The apparent resistivity pseudosection measured over a 2-D model (Fig. 7a) representing a lateral variation in resistivity (Fig. 7b) resembles that for a basement horst as shown in Fig. 7d. The F-ratio between the two pseudosection is 1.434 which is not statistically significant.

A summary of the F-ratio obtained in the various 2-D models is presented in Table 1.

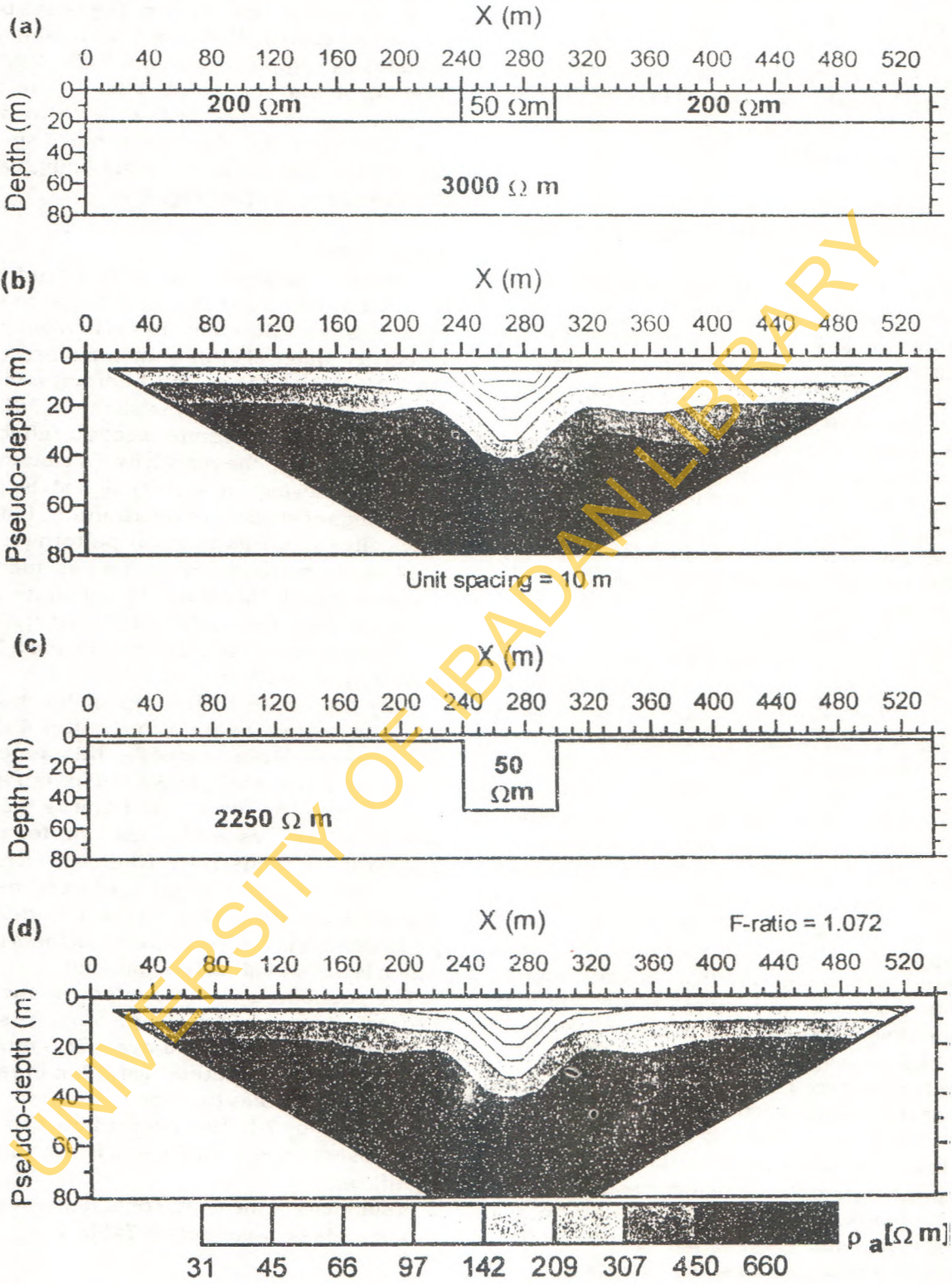


Fig. 4. Equivalence of 2-D models with two vertical contacts (Wenner array), (a) 2-D model with lateral variation in resistivity, (b) apparent resistivity pseudosection calculated from (a), (c) 2-D model that is equivalent to the model in (a), (d) apparent resistivity pseudosection data calculated from the fault model in (c)

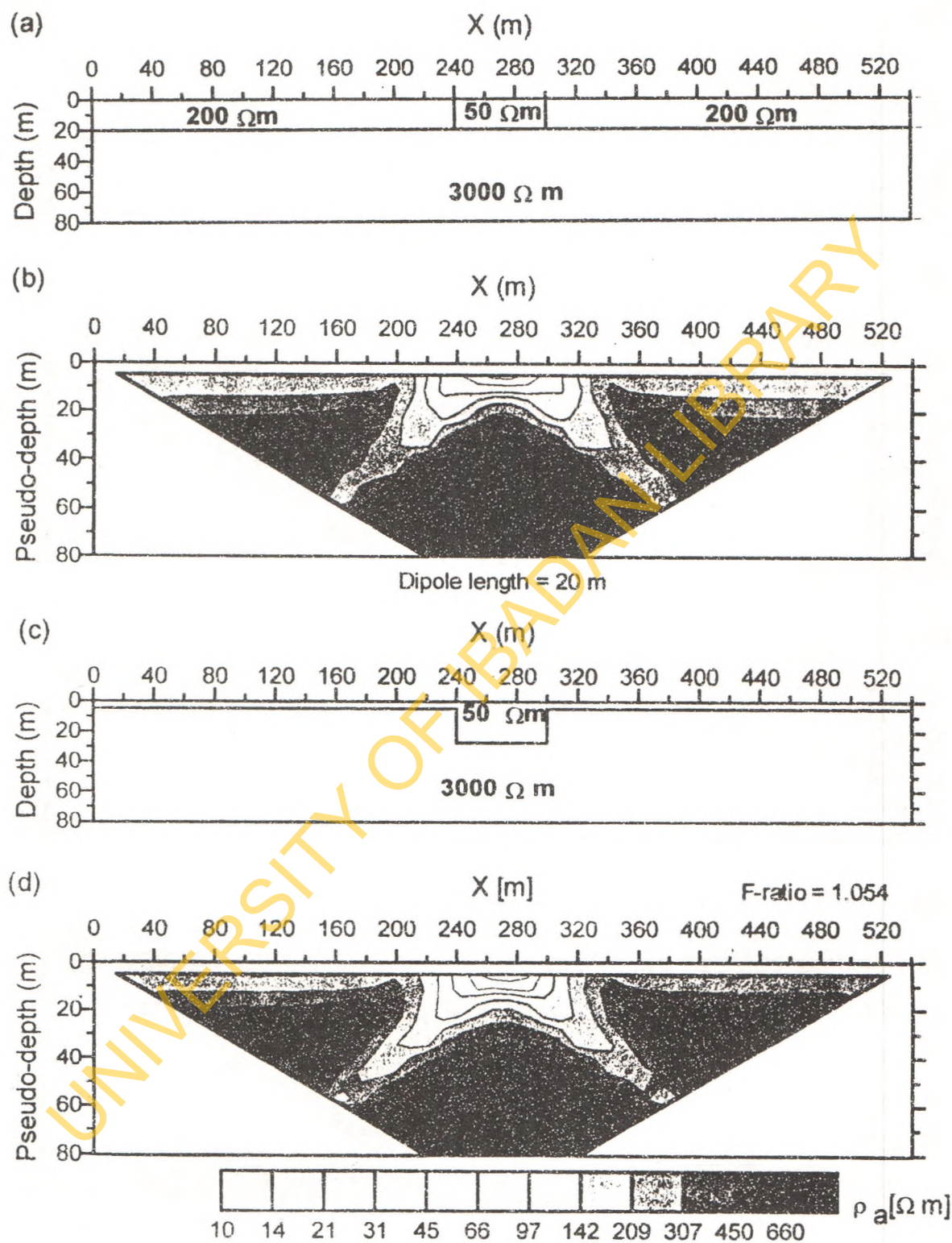


Fig. 5. Equivalence of 2-D models with two vertical contacts (Dipole-dipole array), (a) 2-D model with lateral variation in resistivity, (b) apparent resistivity pseudosection calculated from (a), (c) 2-D model that is equivalent to the model in (a), (d) apparent resistivity pseudosection data calculated from the fault model in (c)

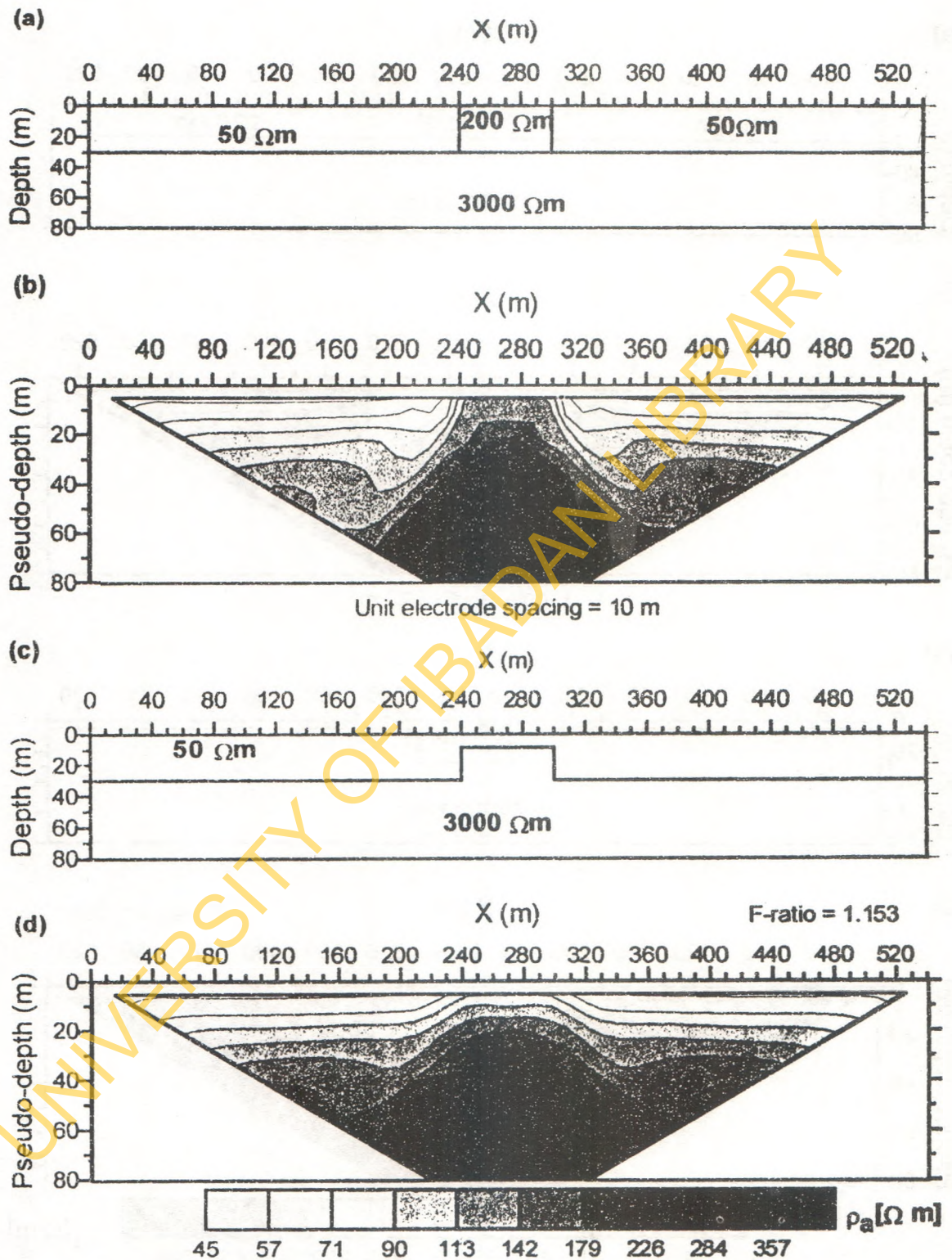


Fig. 6. Example equivalence in a basement horst structure (Wenner array), (a) 2-D model with lateral variation in resistivity, (b) apparent resistivity pseudosection calculated from (a), (c) 2-D model that is equivalent to the model in (a), (d) apparent resistivity pseudosection data calculated from the fault model in (c)

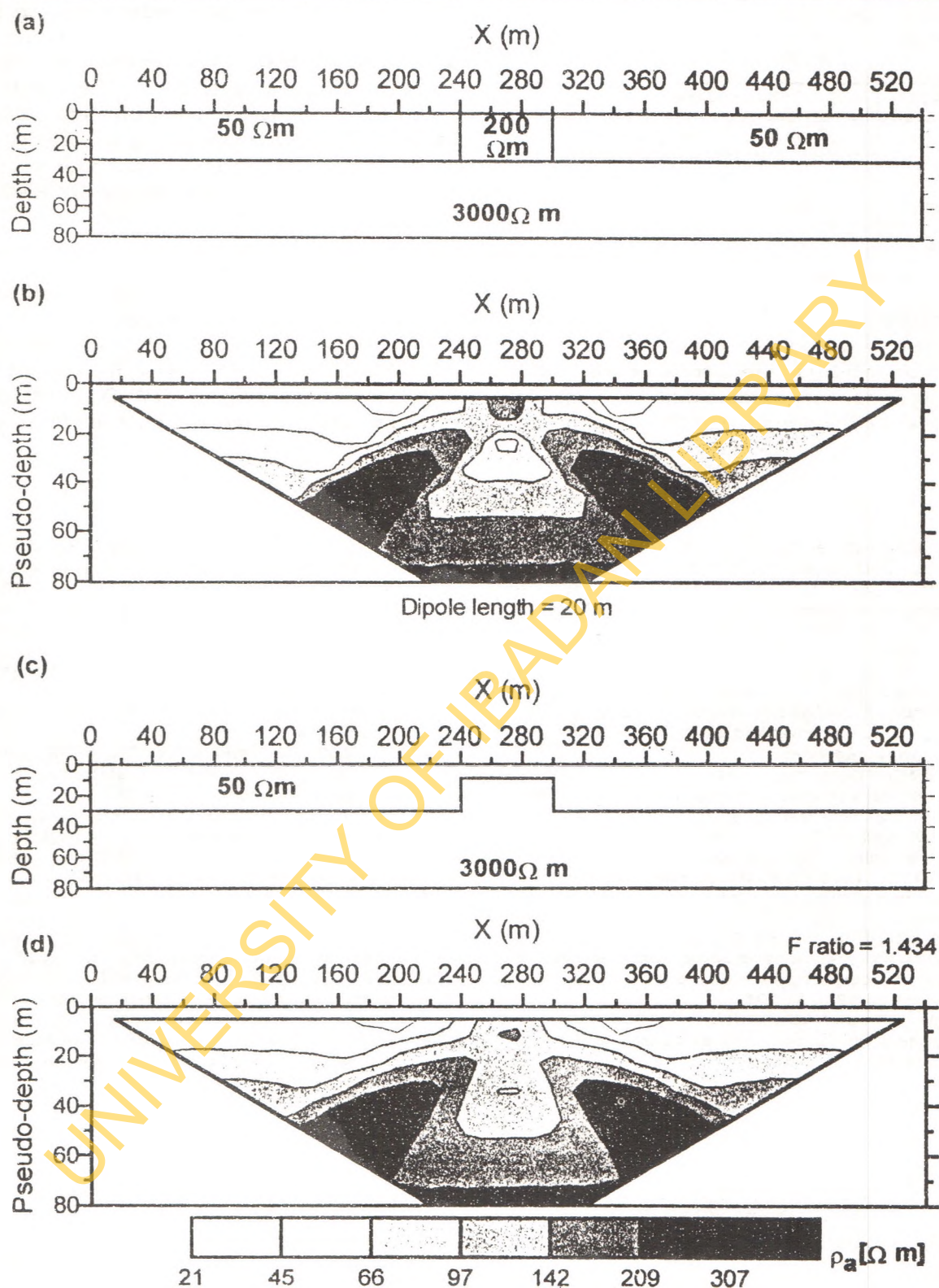


Fig. 7. Equivalence in a basement horst structure (Dipole-dipole array), (a) 2-D model with lateral variation in resistivity, (b) apparent resistivity pseudosection calculated from (a), (c) 2-D model that is equivalent to the model in (a), (d) apparent resistivity pseudosection data calculated from the fault model in (c)

Table 1. Summary of F-values calculated in determining 2-D equivalence between models in this work.

Model	F-calculated	
	Wenner	Dipole-dipole
Fault	1.311	1.304
Trough	1.072	1.054
Horst	1.153	1.434

CONCLUSIONS

It has been shown in this paper that different subsurface models can produce apparent resistivity pseudosection data that are identical, or near-identical enough that they cannot be

differentiated, especially under field conditions when some amount of noise contamination could always be expected. This ambiguity creates a corresponding ambiguity in the depth and structure. As a result, in areas of lateral resistivity variations we cannot always rely on resistivity data alone to resolve the structure. With resistivity tomographic analysis this can be done with the implementation of inversion constraints.

ACKNOWLEDGEMENTS

This study was carried out at the Institute for Geophysics and Meteorology, Technical University, Braunschweig, while the author was on a study visit sponsored by the German Academic Exchange Service (DAAD). P. Weidelt and A. Weller are thanked for encouragement and support.

REFERENCES

- BARKER, R.D., 1992. A simple algorithm for subsurface imaging. *First Break*, 10, 53-62.
- BERNSTONE, C. and DAHLIN, T., 1997. DC resistivity mapping of old landfills: two case studies. *European Journal of Environmental and Engineering Geophysics*, 2, 121-136.
- DAHLIN, T., 1993. On the automation of 2D resistivity surveying for engineering and environmental applications. PhD thesis, Lund University, 187pp.
- DAVIS, J.C., 1973. *Statistical and data analysis in geology*. John Wiley and Sons.
- DEY, A. and MORRISON, H. F., 1979. Resistivity modelling for arbitrarily-shaped two-dimensional structures. *Geophysical Prospecting*, 27, 107-136.
- DRAPER, N.R. and SMITH, H., 1981. *Applied regression analysis*. John Wiley and Sons.
- EDWARDS, L.S., 1977. Modified pseudosection for resistivity and induced polarization. *Geophysics*, 42, 1020-1036.
- GRIFFITHS, D.H. and BARKER, R.D., 1993. Two-dimensional resistivity imaging and modelling in areas of complex geology. *Journal of Applied Geophysics*, 29, 211-226.
- GRIFFITHS, D.H. and TURNBULL, J., 1985. A multi-electrode array for resistivity surveying. *First Break*, 3(7), 16-20.
- GRIFFITHS, D.H., TURNBULL, J. and OLAYINKA, A.I., 1990. Two-dimensional resistivity mapping with a computer-controlled array. *First Break*, 8, 121-129.
- KOEFOD, O., 1979. *Geosounding principles 1: resistivity sounding measurements*. Elsevier Science Publishing Co.
- LOKE, M. H. and BARKER, R.D., 1996. Rapid least-squares inversion of apparent resistivity pseudosection using a quasi-Newton method. *Geophysical Prospecting*, 44, 133-152.
- LOWRY, T., ALLEN, M.B. and SHIVE, P.N., 1989. Singularity removal: a refinement of resistivity modelling techniques. *Geophysics*, 54, 766-774.
- OLAYINKA, A.I. and BARKER, R.D., 1990. Borehole siting in crystalline basement areas of Nigeria with a microprocessor-controlled resistivity traversing system. *Ground Water*, 28, 178-183.
- SIMMS, J. E. and MORGAN, F. D. 1992. Comparison of four least-squares inversion schemes for studying equivalence in one-dimensional resistivity interpretation. *Geophysics*, 57, 1282-1293.
- WELLER, A., SEICHTER, M. and KAMPE, A., 1996. IP modelling using complex electrical conductivities. *Geophysical Journal International*, 127, 387-398.
- ZHDANOV, M.S. and KELLER, G.V., 1994. *The geoelectrical methods in geophysical exploration*. Elsevier Science.